Research Paper

Catalytic oxidant scavenging by selenium-containing compounds: Reduction of selenoxides and *N*-chloramines by thiols and redox enzymes

Luke Carroll[a,b,c], David I. Pattison[a,b], Shanlin Fu[d], Carl H. Schiesser[e], Michael J. Davies[a,b,c], Clare L. Hawkins[a,b,c,*]

[a] *The Heart Research Institute, 7 Eliza St, Newtown, NSW 2042, Australia*
[b] *Sydney Medical School, University of Sydney, Sydney, NSW 2006, Australia*
[c] *Department of Biomedical Sciences, Panum Institute, University of Copenhagen, Blegdamsvej 3, Copenhagen N 2200, Denmark*
[d] *University of Technology Sydney, Centre for Forensic Science, Ultimo, NSW 2007, Australia*
[e] *School of Chemistry and Bio21 Molecular Science and Biotechnology Institute, University of Melbourne, Victoria 3010, Australia*

ARTICLE INFO

ABSTRACT

Myeloperoxidase produces strong oxidants during the immune response to destroy invading pathogens. However, these oxidants can also cause tissue damage, which contributes to the development of numerous inflammatory diseases. Selenium containing compounds, including selenomethionine (SeMet) and 1,4-anhydro-5-seleno-D-talitol (SeTal), react rapidly with different MPO-derived oxidants to form the respective selenoxides (SeMetO and SeTalO). This study investigates the susceptibility of these selenoxides to undergo reduction back to the parent compounds by intracellular reducing systems, including glutathione (GSH) and the glutathione reductase and thioredoxin reductase systems. GSH is shown to reduce SeMetO and SeTalO, with consequent formation of GSSG with apparent second order rate constants, k_2, in the range 10^3–$10^4\,M^{-1}\,s^{-1}$. Glutathione reductase reduces both SeMetO and SeTalO at the expense of NADPH via formation of GSSG, whereas thioredoxin reductase acts only on SeMetO. The presence of SeMet and SeTal also increased the rate at which NADPH was consumed by the glutathione reductase system in the presence of *N*-chloramines. In contrast, the presence of SeMet and SeTal reduced the rate of NADPH consumption by the thioredoxin reductase system after addition of *N*-chloramines, consistent with the rapid formation of selenoxides, but only slow reduction by thioredoxin reductase. These results support a potential role of seleno compounds to act as catalytic scavengers of MPO-derived oxidants, particularly in the presence of glutathione reductase and NADPH, assuming that sufficient plasma levels of the parent selenoether can be achieved in vivo following supplementation.

1. Introduction

Neutrophils are key effector cells of the innate immune response, and are responsible for the release of bactericidal enzymes, including myeloperoxidase (MPO), and the generation of powerful oxidants to destroy invading pathogens [1,2]. MPO is a heme enzyme that catalyzes the reaction between hydrogen peroxide (H_2O_2) and halide and pseudohalide ions (chloride, Cl⁻; bromide, Br⁻; thiocyanate, SCN⁻) to produce the corresponding hypohalous acids, hypochlorous acid (HOCl), hypobromous acid (HOBr) and hypothiocyanous acid (HOSCN)

[1,3]. HOCl and HOBr react with amines to form the secondary oxidants *N*-halamines, which can retain the oxidizing capacity of the parent oxidants [1,4]. Although all of these species are effective in controlling or destroying pathogens, they are also capable of causing host tissue damage, and have been associated with many inflammatory diseases, including atherosclerosis, neurodegeneration, arthritis, kidney disease and some cancers [1,5]. Given the strong association between the generation of MPO oxidants in vivo and the development of inflammatory disease, there is significant interest in developing novel scavengers and / or inhibitors, which may be of therapeutic benefit

(reviewed [6]).

Selenium-containing compounds, including selenomethionine (SeMet) and 1,4-anhydro-5-seleno-D-talitol (SeTal), are potential candidates to limit oxidative damage during inflammation *in vivo*, on account of their high reactivity with a number of key biological oxidants, including HOCl, HOBr, HOSCN, *N*-chloramines, H_2O_2 and peroxynitrous acid (ONOOH) [7-11]. The second-order rate constants for these reactions are some of the highest reported for biologically relevant reactions [7-11]. The reaction of SeMet with oxidants results primarily in the formation of selenomethionine selenoxide (SeMetO), which can be subsequently reduced by thiols such as glutathione (GSH) (Reaction 1) [7,11-15]. Other selenoxides formed on reaction of Se compounds with H_2O_2, can also be reduced by GSH, regenerating the parent Se compound and forming GSSG [16,17], which provides a pathway for potentially catalytic oxidant scavenging.

The reaction of SeMet with oxidants results primarily in the formation of selenomethionine selenoxide (SeMetO), which can be subsequently reduced by thiols such as glutathione (GSH) (Reaction (1)) [7,11,14–17]. Other selenoxides formed on reaction of Se compounds with H_2O_2, can also be reduced by GSH, regenerating the parent Se compound and forming GSSG [18,19], which provides a pathway for potentially catalytic oxidant scavenging.

$$SeMetO + 2GSH \rightarrow SeMet + GSSG + H_2O \qquad (1)$$
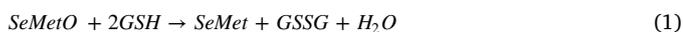
Glutathione reductase (GSR) regenerates GSH from GSSG at the expense of NADPH, which potentially links oxidant removal with NADPH consumption and cellular metabolism [20]. Whilst evidence has been presented previously for selenoxide reduction by GSH [14,21], the mechanisms and rate constants for these reactions have not been reported. For rapid detoxification of oxidants and prevention of selenoxide accumulation, which would arrest the reduction cycle, it is critical for these rate constants to be of a high value and hence competitive with the initial reactions resulting in selenoxide formation.

SeMetO can also be reduced enzymatically, via the action of thioredoxin reductase (TrxR) and thioredoxin (Trx) (Reaction (2)) [21]. There is evidence that other Se compounds, including ebselen, selenocystamine and diselenides, can interact with TrxR [22,23], which allows catalytic reduction of peroxides and ONOOH [21–23]. This detoxification pathway may extend to MPO-derived oxidants, including HOCl and *N*-chloramines, that react rapidly with the Se compounds SeMet and SeTal, forming selenoxides [11].

$$SeMetO + NADPH \xrightarrow{TrxR} SeMet + NADP^+ + H_2O \qquad (2)$$

The aim of this study was therefore to assess the catalytic oxidant scavenging potential of SeMet and SeTal by determining rate constants for the reduction of the corresponding selenoxides by GSH, and investigating the interaction between the selenoxides and the enzymatic reductants GSR and TrxR in the presence of NADPH. The study was subsequently extended to assess whether catalytic removal of *N*-chloramines could also be mediated by SeMet and SeTal in the presence of GSR and TrxR. The resulting data support the possibility of supplementation with Se compounds as way to reduce oxidative damage during chronic inflammatory conditions.

2. Materials and methods

2.1. Materials

All buffers, and solutions where indicated, were prepared using nanopure water filtered through a four-stage Milli-Q system (Millipore Waters, Australia). Solutions were prepared in 0.1 M, pH 7.4, phosphate buffer, unless otherwise specified. HOCl was prepared by dilution of a concentrated stock solution of NaOCl (12.5% w/v; Ajax FineChem Ltd, Australia), standardised at pH 12 by UV absorbance at 290 nm ($\varepsilon = 350$ M^{-1} cm^{-1} [24]). SeMet and methylselenocysteine were from

Sigma-Aldrich (Castle Hill, NSW, Australia), and 1,4-anhydro-4-seleno-D-talitol (SeTal) was synthesised as described previously [25]. *N*-acetylselenomethionine was kindly prepared by Dr Lara Malins and seleno-bis-propionic acid was kindly provided by Prof. Indira Priyadarshini. Selenoxides (SeMetO, SeTalO, *N*-acetylselenomethionine selenoxide (NASMO), seleno-bis-propionic acid selenoxide (SePropO) and methylselenocysteine selenoxide (MSCO)) were prepared by mixing the parent Se compound (4 mM) with an equal volume of H_2O_2 (2 mM; Merck, Bayswater, VIC, Australia) with incubation for 10 min at 21 °C before dilution to the desired concentration in phosphate buffer (0.1 M, pH 7.4).

2.2. Thiol quantification

The consumption of GSH (4 μM) on addition of SeMetO and SeTalO (0–1 μM) was assessed by measuring the change in fluorescence ($\lambda_{ex} = 360$ nm; $\lambda_{em} = 530$ nm) of ThioGlo-1 using an M2e plate reader (Molecular Devices) as described previously [26]. The thiol concentrations were determined by comparison of the fluorescence intensity to a standard curve prepared using GSH (0–5 μM).

2.3. N-Chloramine formation and quantification

N-chloramines were prepared by reaction of taurine (Tau), glycine (Gly) or *N*-α-acetyllysine (Lys) (10 mM) with HOCl (2 mM). *N*-chloramine concentrations were determined by measuring 5-thio-2-nitrobenzoic acid (TNB) consumption at 412 nm as described previously [26], using an extinction coefficient $\varepsilon = 14,150$ cm^{-1} [27].

2.4. Stopped-flow kinetics

Stopped flow kinetics experiments were carried out using an Applied Photophysics SX.20MV stopped flow system maintained at 22 °C using a thermostatted water bath. The detection system consisted of an Xe light source (150 W; Osram GmbH, Munich, Germany) with wavelength selection achieved using a single monochromator (slit width, 0.5 mm; bandwidth, ± 1.2 nm) and photomultiplier detection. The system was controlled by a computer running Pro-Data SX (version 2.2.12; Applied Photophysics). Spectral data from 200 to 310 nm were obtained by acquiring kinetic traces at 10 nm intervals with the photomultiplier over this wavelength region. Second-order rate constants were typically obtained by global analysis of the kinetic traces using second order models with λ > 240 nm using ProKIV (Applied Photophysics, Version 1.0.1.4), although in some cases it was more appropriate to apply pseudo-first order analysis at selected wavelengths to derive the rate constants.

2.5. Enzymatic NADPH consumption

The reduction of each selenoxide (200 μM) by TrxR (25 nM; IMCO, Stockholm, Sweden) was assessed by measuring the change in absorbance of NADPH (700 μM; Roche, Castle Hill, NSW, Australia) at 340 nm every 30 s for 2 h using a M2e plate reader (Molecular Devices). The rate of consumption of NADPH (700 μM) was also used to assess the effect of SeMet and SeTal (20–200 μM) on the rate of *N*-chloramine (200 μM) reduction by TrxR (25 nM). An Applied Photophysics SX.20MV stopped flow system was used to quantify NADPH (500 μM) loss upon addition of each selenoxide (200 μM) to GSR (25 nM) and GSH (400 μM) in phosphate buffer (pH 7.4, 0.1 M). *N*-Chloramine (200 μM) reduction experiments were also performed by addition of SeMet or SeTal (20–200 μM) prior to exposure of the resulting solution to the NADPH/GSR/GSH mixture. For the GSR experiments, the loss of NADPH was measured by monitoring the absorbance of 340 nm over 60 s with a linear slope fitted to the initial decrease in absorbance, over 2–10 s, where maximum enzymatic activity was observed.

2.6. Selenoxide quantification by HPLC

Separation of SeMet and SeMetO was achieved by injection of each sample (20 µL) onto a Beckman Ultrasphere ODS column (5 µm, 4.6×250 mm) at 40 °C with an isocratic elution method with a flow rate of 1 mL min^{-1} using acetonitrile (1% v/v) adjusted to pH 2.5 with trifluoroacetic acid (TFA; 0.005% v/v) as described previously [17]. SeMet and SeMetO eluted at 3.2 min and 8.6 min respectively, and were quantified by measuring the absorbance at 220 nm using a photodiode array detector (SPD-M20A, Shimadzu). The separation of SeTal and SeTalO was achieved by injecting samples (20 µL) onto an Agilent Zorbax carbohydrate column (5 µm, 4.6×150 mm) at 35 °C. The samples were eluted with an isocratic elution method with a flow rate of 1 mL min^{-1} using acetonitrile (75% v/v) acidified with TFA (0.005% v/v) for 8 min, followed by a washing step whereby the H$_2$O content in the acetonitrile mobile phase was increased to 75% (v/v) over 1 min, followed by elution for 3.5 min, before reducing the H$_2$O content to 25% over 1 min, and re-equilibration for 2.5 min. SeTal and SeTalO eluted at 2.7 min and 4.4 min respectively, and were quantified at 220 nm as described above. Samples (20 µL) containing NADPH from the enzymatic reduction assays were injected onto an Agilent Zorbax 300SCX column (5 µm, 4.6×250 mm) at 30 °C and eluted using an isocratic method with a mobile phase of NaH$_2$PO$_4$ (0.01 M, pH 4.8) and a flow rate of 1 mL min^{-1}. Under these conditions, the retention times for SeMet, SeMetO, SeTal and SeTalO were 3.9 min, 4.4 min, 3.4 min and 3.7 min, respectively, with quantification by measuring absorbance at 220 nm.

2.7. Statistical analyses

Data are expressed as mean ± standard deviation (SD) from at least 3 independent experiments, with statistical analyses performed using one-way ANOVA with Tukey's post-hoc testing (GraphPad Prism 6, GraphPad Software, San Diego, USA), with $p < 0.05$ taken as a significant.

3. Results

3.1. Reduction of SeMet and SeTal selenoxides by GSH

Addition of increasing concentrations of SeMetO (0–1 µM, black bars) or SeTalO (0–1 µM, grey bars) to GSH (4 µM) resulted in a dose-dependent decrease in GSH concentrations as assessed using the ThioGlo-1 assay (Fig. 1a). The reduction of SeMetO and SeTalO (1.6 mM), and regeneration of SeMet and SeTal in the presence of GSH (0–3.2 mM) were subsequently assessed by HPLC methods. The concentration of SeMetO decreased in a dose-dependent manner upon incubation with increasing concentrations of GSH, which resulted in a corresponding increase in the concentrations of SeMet and GSSG (Fig. 1b and d). The stoichiometry observed for this reaction was ca. 2:1 for GSH and SeMetO, with every 0.2 mM of SeMetO consumed resulting in 0.2 mM SeMet and GSSG, with the consumption of 0.4 mM GSH, in accord with previous studies [14,15]. Similar behaviour was observed in the corresponding studies with SeTalO (1.6 mM) and GSH (0–3.2 mM) (Fig. 1c), though in this case, quantification of GSSG was not possible due to interferences in the HPLC method.
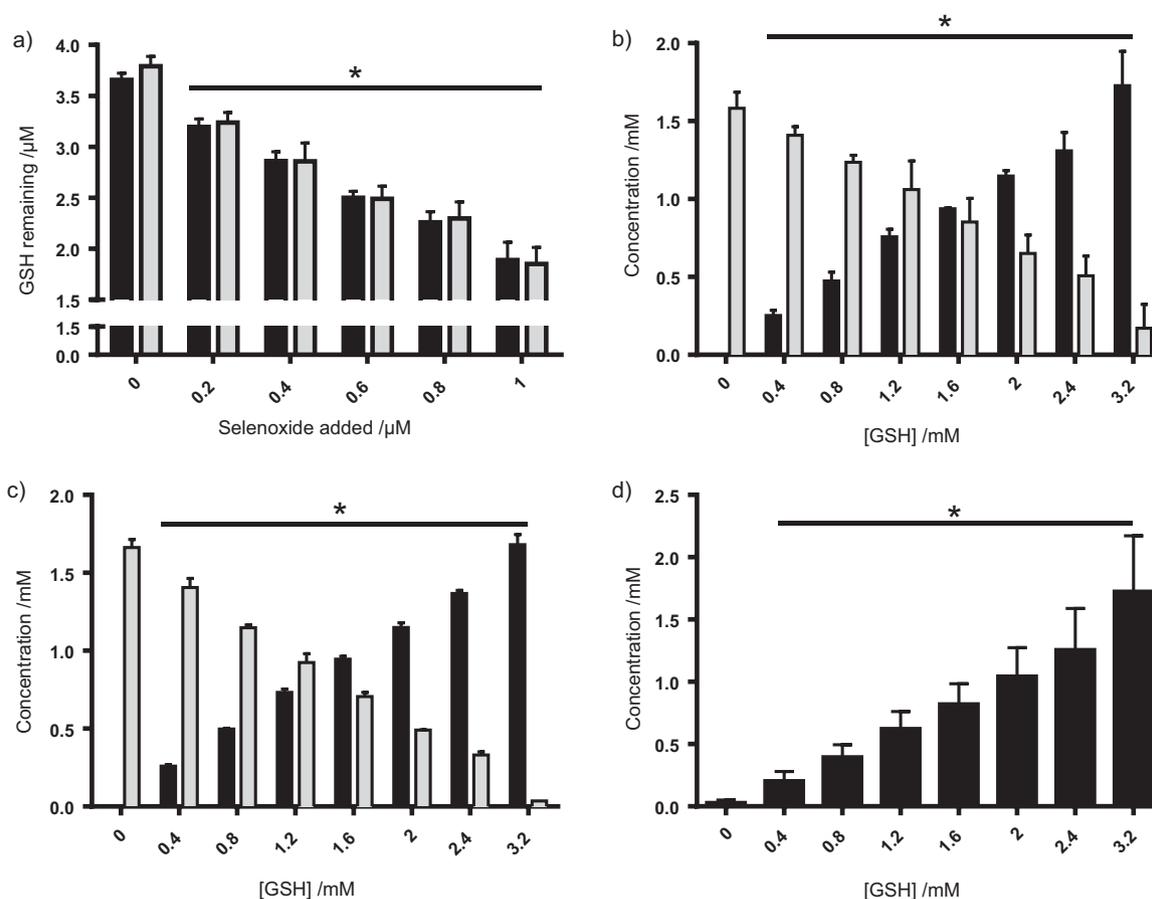
Fig. 1. Selenoxides formed on SeMet and SeTal consume GSH to produce GSSG and the parent SeMet or SeTal. (a) SeMetO (black bars) or SeTalO (grey bars) (0–1 µM) was added to GSH (4 µM) and incubated for 10 min before remaining thiol was assessed by the ThioGlo assay. (b–d) GSH (0–3.2 mM) was added to (b,d) SeMetO (1.6 mM) or (c) SeTalO (1.6 mM) and incubated for 10 min before analysis by HPLC and determination of concentrations of (b) SeMetO (grey bars) and SeMet (black bars), (c) SeTalO (grey bars) and SeTal (black bars), and (d) GSSG. Data represent mean ± SD from 3 independent experiments. * indicates significant difference ($p < 0.05$) from the corresponding control where no selenoxide or GSH were added, by one-way ANOVA with Tukey's post-hoc test.
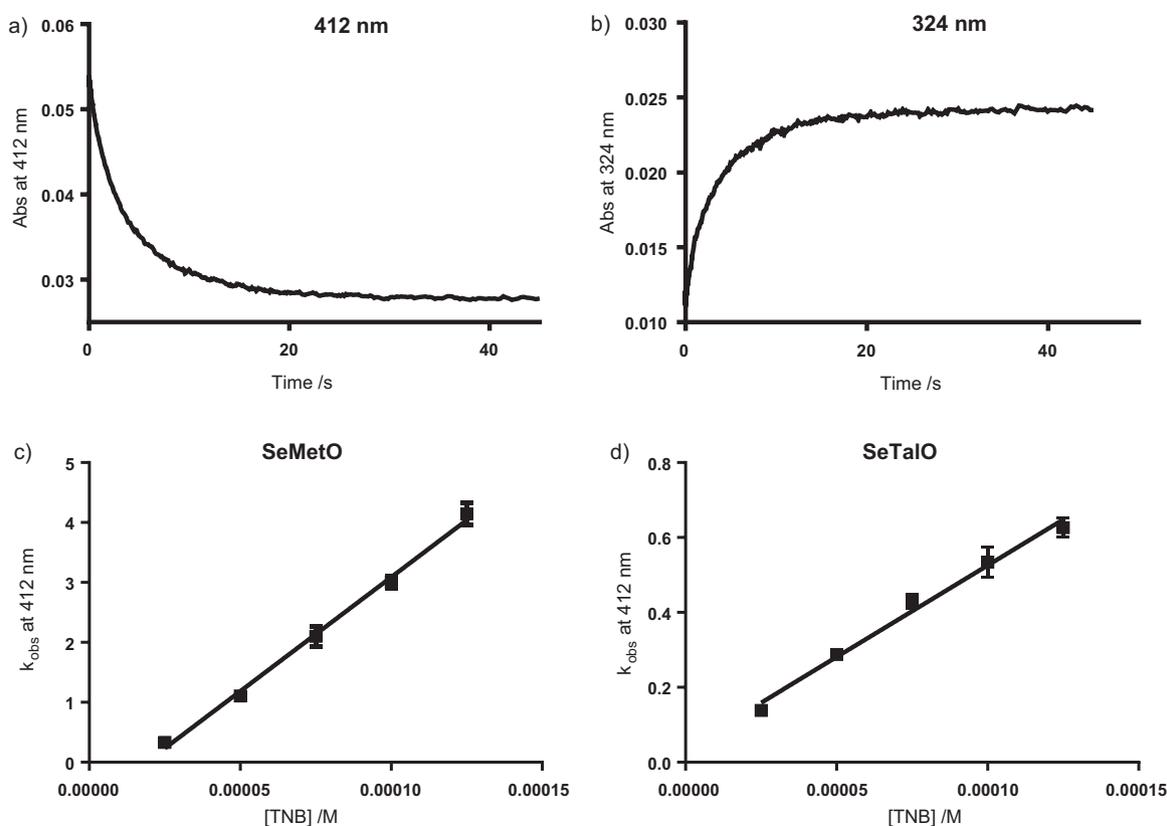
Fig. 2. Kinetic analysis of the reduction of SeMetO by TNB. (a,b) Stopped flow kinetic traces measured for SeMetO (5 μM) and TNB (25 μM) in phosphate buffer (pH 7.4, 0.1 M) using a 2 mm path length cell at 22 °C measured at (a) 412 and (b) 324 nm. A loss in absorbance was observed at 412 nm, indicating TNB consumption, with a concomitant increase in absorbance at 324 nm, indicating DTNB formation. (c,d) The observed rate constants, k_{obs}, were determined from the kinetic plots and k_{obs} was plotted against the initial TNB concentration for (c) SeMetO or (d) SeTalO. Data represent mean ± SD of three independent experiments.

3.2. Second order rate constants for the reaction of selenoxides with thiols

Initial studies were performed using TNB as a model thiol, as TNB and the disulfide product 5,5′-dithiobis-(2-nitrobenzoic acid) (DTNB) have absorbance maxima at 412 nm and 324 nm respectively, which are distinct from the absorbance profiles of the selenoxides, which simplifies the kinetic analysis. SeMetO (5 μM) was mixed with increasing concentrations of TNB (25–125 μM) and the absorbance monitored at 324 or 412 nm over 45 s by stopped flow apparatus. A rapid decrease in absorbance at 412 nm was observed (Fig. 2a), indicating TNB consumption, with a concomitant increase in absorbance at 324 nm (Fig. 2b), indicating DTNB formation. These changes are consistent with the reaction of SeMetO with TNB to give SeMet and DTNB. Similar results were obtained with SeTalO. In each case, the absorbance changes could be satisfactorily analysed in terms of a pseudo first-order mechanism, with single exponential curves fitting well to the experimental data. These fits

yielded k_{obs} for each condition, with the second-order rate constants obtained from the linear plots of k_{obs} against the initial concentration of TNB (Fig. 2c and d for SeMetO and SeTalO; Table 1).

Complementary analyses were undertaken by converting the raw kinetic data into linear plots of ln(Abs) vs time; these plots yielded very similar k_{obs} values. With both SeMetO and SeTalO, the consumption of TNB occurs with the same rate constant as the production of DTNB, suggesting that the mechanism involves initial reaction of one molecule of TNB with the selenoxide with a second order rate constant k_1, followed by reaction with a second TNB molecule with a second-order rate constant k_2, to produce the reduced Se compound and DTNB as products (Scheme 1). We also performed kinetic modelling studies that demonstrated that in a 2-step system where the $k_2 > k_1$ (for modelling purposes a 10-fold increase of k_1 over k_2 was used), the thiol concentration [RSH] decreased exponentially and the first-order plot was linear (Supplementary material Fig. S1). k_1 could then be deter-

Table 1
Second-order rate constants for the reduction of selenoxides by TNB.

	Rate constants for the reduction of selenoxides by thiols ($M^{-1} s^{-1}$)			
Selenoxide	TNB[a]	DTNB[b]	TNB[a] in the presence of 10 mM Gly	GSH[c]
SeMetO	$(3.8 \pm 0.1) \times 10^4$	$(3.8 \pm 0.1) \times 10^4$	–	$k_1 = (1.2 \pm 0.4) \times 10^5$ and $k_2 = (1.5 \pm 0.2) \times 10^4$
SeTalO	$(4.9 \pm 0.2) \times 10^3$	$(4.8 \pm 0.2) \times 10^3$	–	$(3.4 \pm 0.3) \times 10^3$
MSCO	$(4.4 \pm 0.3) \times 10^3$	$(4.9 \pm 0.6) \times 10^3$	$(5.0 \pm 0.3) \times 10^3$	$(2.5 \pm 0.4) \times 10^4$
NASMO	$(1.2 \pm 0.1) \times 10^3$	$(1.2 \pm 0.1) \times 10^3$	$(2.5 \pm 0.2) \times 10^3$	$(1.3 \pm 0.2) \times 10^3$
SePropO	$(1.3 \pm 0.1) \times 10^3$	$(1.31 \pm 0.06) \times 10^3$	–	$(4.6 \pm 0.6) \times 10^2$

[a] Rate constant, k, for loss of thiol.
[b] Rate constant, k, for formation of disulfide.
[c] Rate constant designated k_1 represents the reaction of the thiol with selenoxide to form a selenosulfide, with k_2 representing reaction of the selenosulfide with a second thiol to produce the disulfide and selenoether.
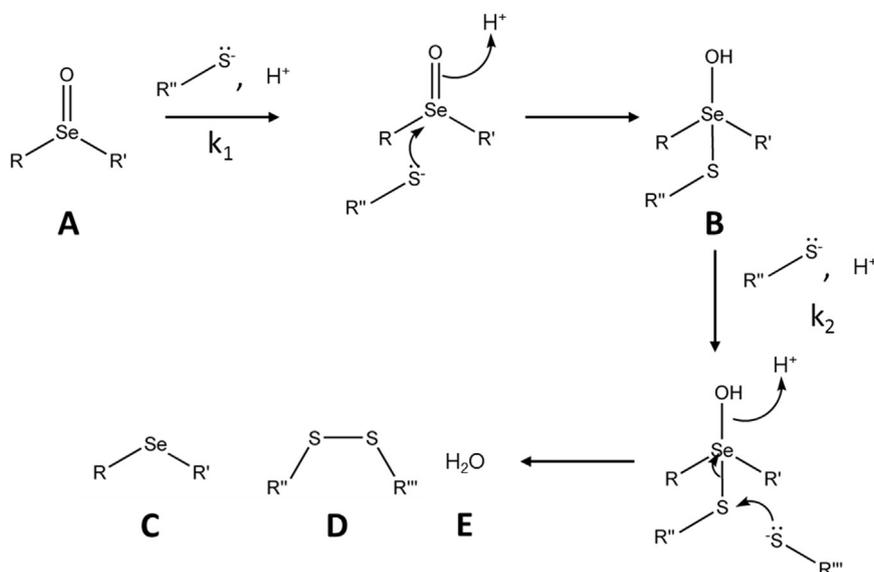
Scheme 1. Proposed two-step mechanism of selenoxide reduction by thiols. Initial reaction of selenoxides (A) with thiols is proposed to lead to the formation of a seleno-sulfide intermediate (B). The rate constant for the initial reaction is designated as k_1. A second thiol then reacts with the intermediate with a rate constant k_2, producing a selenoether (C), disulfide (D) and water (E) as products.

mined from the gradient of the pseudo first-order plot. However, if $k_1 > k_2$, 2-phase kinetics would be observed for [RSH]. This gives a non-linear first-order plot, and a single exponential decay does not fit to the data well (Supplementary material Fig. S1).

The second-order rate constant determined for SeMetO with TNB is ca. 10-fold greater than that observed for SeTalO (Table 1). This is believed to arise from interaction of the Se centre with the lone pair of electrons of the nitrogen atom of the amine group. Such Se-N interactions are known to affect the rates of reduction and oxidation of other Se species [22,23]. Consequently, a range of other selenoxides were examined, including the oxides of methylselenocysteine (MSCO), *N*-acetylselenomethionine (NASMO) and seleno-bis-propionic acid (Se-PropO) (Fig. 3), where such interactions would be expected to be modulated. k_{obs} values were determined at 412 nm from analysis of kinetic data obtained on mixing the selenoxides (5 µM) with TNB (25–125 µM) using single exponential fitting (Supplementary material Fig. S2; Table 1). The determined rate constants for reduction were decreased by ~10-fold compared to SeMetO, when there was a shorter carbon chain between the Se and the amine (MSCO), on acetylation of the amine (NASMO) or removal of the amine (SePropO).

The effect of Se-N interactions was further examined by determining the second-order rate constants for reduction of the selenoxides MSCO and NASMO by TNB in phosphate buffer (0.1 M, pH 7.4) supplemented with Gly (10 mM), as an extramolecular source of amine. The k_2 value for MSCO under these conditions was essentially unchanged compared to the absence of Gly (Supplementary material Fig. S2, Table 1), whereas that for NASMO was significantly increased in the presence of Gly, suggesting that Se-N interactions may promote selenoxide reduction by thiols.

Analogous studies were performed to assess the reactivity of SeMetO, SeTalO and other selenoxides (125 µM) with GSH (0.5–2.5 mM) by monitoring absorbance changes by stopped flow at wavelengths between 240 and 300 nm (at 10 nm intervals). For SeTalO, MSCO, NASMO and SePropO, increases in absorbance across these wavelengths were observed (data for SeTalO shown in Fig. 4a and b). The observed changes in absorbance yielded a linear plot of ln(Abs) vs time, and could be fitted to a single exponential function to yield the k_{obs} values at each GSH concentration. The reported k_2 values for the reduction of SeTalO, MSCO, NASMO and SePropO (Table 1) were determined by global analysis of the absorbance changes from 240 to 300 nm using the mechanism outlined in Reaction (3). These data are

consistent with the initial reaction of the selenoxide being the rate determining step, as seen with TNB.

$$\text{Selenoxide} + \text{RSH} \xrightarrow{k_1} \text{Product} \qquad (3)$$

In contrast, the kinetic traces observed for the reduction of SeMetO by GSH were more complex, with absorbance changes showing two separate phases on mixing SeMetO (125 µM) with GSH (0.5–2.5 mM). Representative kinetic data with GSH (0.5 mM) are shown in Fig 4c and d. At 240 nm, there was a fast initial decrease in absorbance over ca. 20 ms, which was followed by a subsequent increase in absorbance over ca. 200 ms (Fig. 4d). These separate phases were also observed across a range of other wavelengths, but in these cases both phases exhibited increases in absorbance intensity (data not shown). The kinetic data with SeMetO and GSH are consistent with the mechanism proposed in Scheme 1, but with $k_2 < k_1$. The value of k_1 was determined by pseudo first-order analysis of the initial decrease in absorbance observed at 240 nm (Supplementary material Fig. S3). The resulting k_1 value was used during global wavelength analysis of the data to decrease the number of unknown parameters in Reaction (4). These analysis methods yielded values of $k_1 = (1.2 \pm 0.4) \times 10^5 \, \text{M}^{-1} \, \text{s}^{-1}$ and $k_2 = (1.5 \pm 0.2) \times 10^4 \, \text{M}^{-1} \, \text{s}^{-1}$ for the reduction of SeMetO by GSH.

$$\text{Selenoxide} + \text{GSH} \xrightarrow{k_1} \text{Intermediate} + \text{GSH} \xrightarrow{k_2} \text{Products} \qquad (4)$$
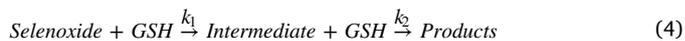
3.3. Reduction of selenoxides by the thioredoxin reductase system

The ability of TrxR to reduce SeMetO and SeTalO was compared, as it has been reported previously that this enzymatic system can reduce SeMetO [21]. The reduction of SeMetO and SeTalO (200 µM) by TrxR (25 nM) in the presence of NADPH (700 µM) was examined by measuring the consumption of the latter at 340 nm (Fig. 5a), with the data obtained over the first 10 min fitted to a straight line. The addition of SeMetO induced an increase in NADPH consumption, but no change was observed with SeTalO (Fig. 5b). The reduction of SeMetO and SeTalO by TrxR was examined further by HPLC to assess the concentration of SeMetO, SeTalO, SeMet and SeTal 2 h after addition of SeMetO or SeTalO to TrxR in the presence of NADPH (700 µM). Evidence was obtained for the complete reduction of the SeMetO, with a corresponding increase in SeMet concentration, whereas no changes in the SeTalO or SeTal concentrations were observed, consistent with the kinetic data. This suggests that while TrxR can reduce SeMetO,
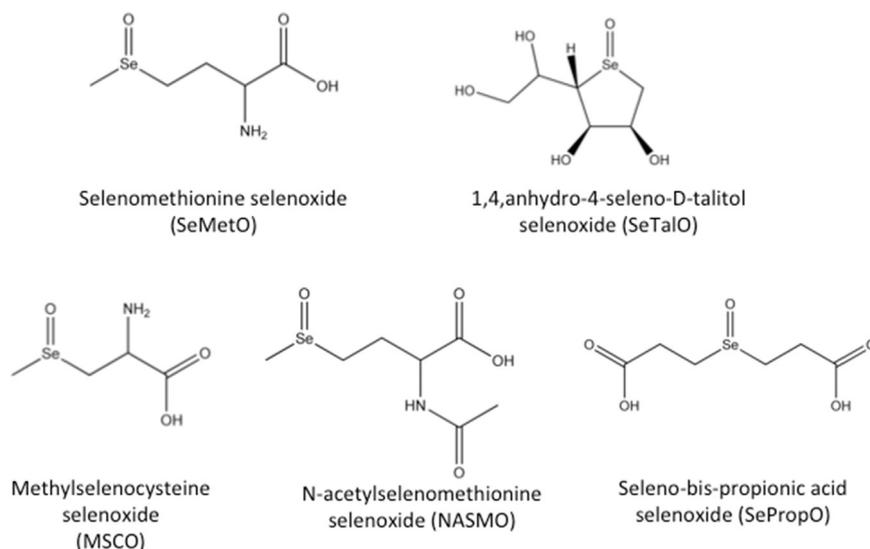
Fig. 3. Structures of selenoxides used in the determination of the mechanisms and kinetics of selenoxide reduction by thiols.

SeTalO is not a substrate.

Experiments were also performed by co-incubating SeMetO and SeTalO with TrxR in the presence of NADPH and other components of cellular reduction and repair systems, including Trx (1.5 µM), glutathione peroxidase (GPx, 1.5 µM) and methionine sulfoxide reductases (MsrA, 95 nM; MsrB2, 0.25 µM). However, inclusion of these enzymes did not increase either the rate of NADPH consumption (assessed by absorbance at 340 nm), or the quantity of selenoxide reduced (as measured by HPLC; data not shown).

3.4. Reduction of selenoxides by the glutathione reductase system

The reduction of selenoxides by GSH results in the formation of GSSG (Fig. 1d), therefore the ability of the GSR system (NADPH/GSR/GSH) to reduce SeMetO and SeTalO was assessed. Given the rapid rate of reaction of selenoxides with GSH, SeMetO and SeTalO (200 µM) were
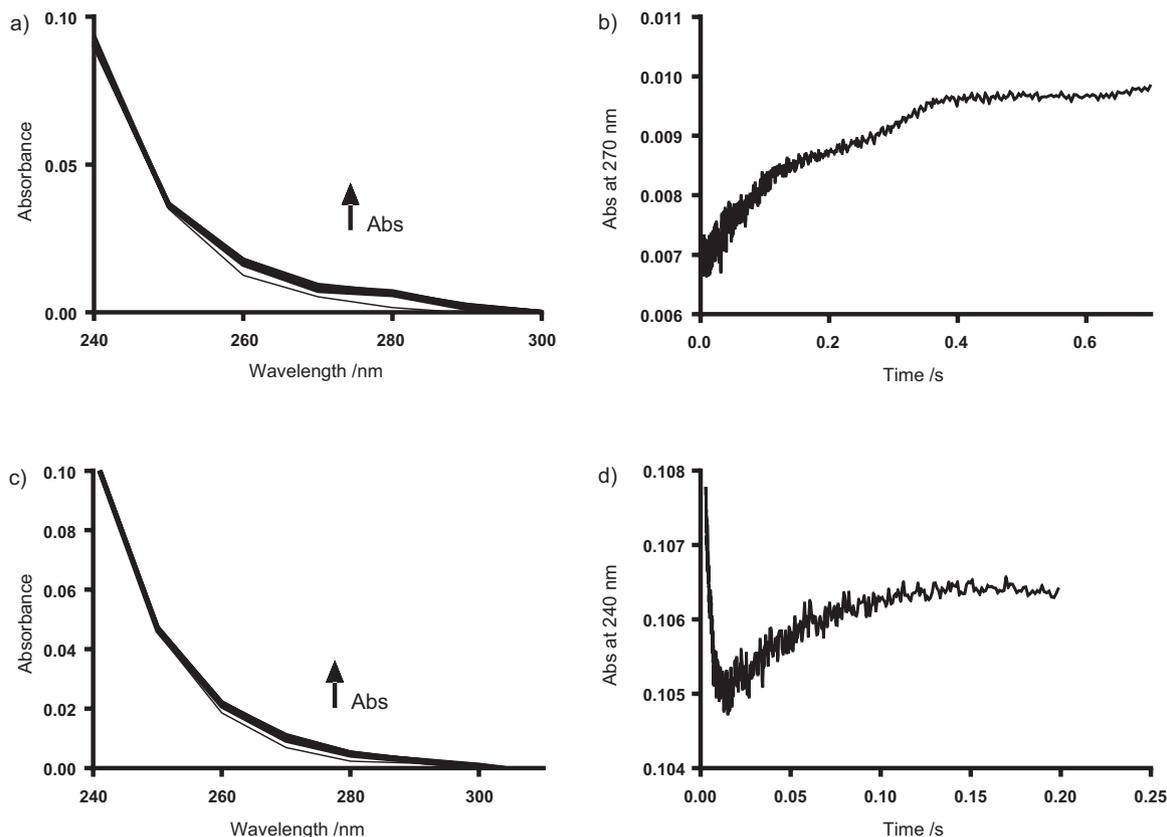
Fig. 4. Stopped flow kinetic data for the reduction of SeTalO and SeMetO by GSH. (a,b) SeTalO (125 µM) was mixed with GSH (0.5 mM) in phosphate buffer (pH 7.4, 0.1 M) at 22 °C using a 10 mm path length cell. (a) shows the absorbance changes over 0.75 s monitored at wavelengths between 240 and 300 nm and (b) shows the absorbance change monitored at 270 nm. (c,d) SeMetO (125 µM) was mixed with GSH (0.5 mM) in phosphate buffer (pH 7.4, 0.1 M) at 22 °C. (c) Shows the absorbance changes over 0.2 s monitored at wavelengths between 240 and 300 nm and (d) shows the absorbance change monitored at 240 nm where two-phase kinetics are observed. Data represent three independent experiments.
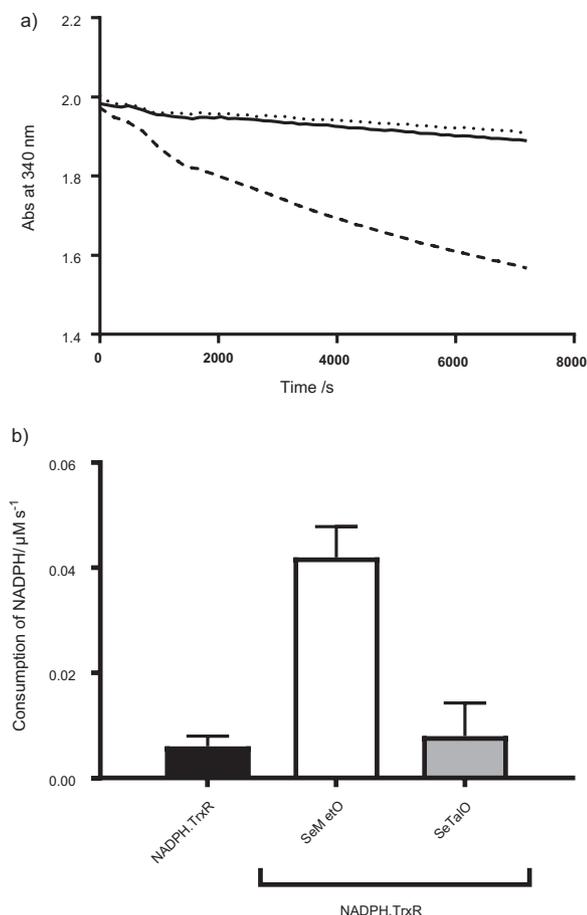
Fig. 5. Enzymatic reduction of SeMetO and SeTalO by the TrxR system. Panel (a) shows typical absorbance changes of NADPH at 340 nm over time with SeMetO (200 μM; dashed line), or SeTalO (200 μM; dotted line) on addition to TrxR (25 nM) and NADPH (700 μM). The absorbance change of the assay mixture in the absence of selenoxide is shown by the solid line. Panel (b) shows the rate of consumption of NADPH by fitting a straight line to the first 10 min of the data represented in (a). For panel (b), data represent mean ± SD from 3 independent experiments.

Fig. 6. Enzymatic reduction of SeMetO and SeTalO by the GSR system. Panel (a) shows typical absorbance changes of NADPH at 340 nm over time with SeMetO (200 μM; dashed line), or SeTalO (200 μM; dotted line) on addition to GSR (25 nM), GSH (400 μM) and NADPH (500 μM) using a stopped-flow system with 2 mm path length cell. Panel (b) shows the initial rate of absorbance decrease over the first 10 s of data represented in (a). For panel (b), data represent mean ± SD from 3 independent experiments.

mixed with the GSR assay mixture (500 μM NADPH, 25 nM GSR and 400 μM GSH) using a stopped flow apparatus to determine the consumption of NADPH at 340 nm over a period of 1 min (Fig. 6a). The initial rate of NADPH consumption was determined by fitting a straight line to the first 10 s of data. NADPH was consumed at a rate of 9.1 ± 1 or 8.3 ± 0.3 mAbs s^{-1} upon mixing SeMetO or SeTalO respectively (Fig. 6b).

In order to confirm that NADPH consumption reflects recycling of the GSSG by GSR following SeMetO reduction by GSH, SeMetO (200 μM) was incubated with the GSR system (500 μM NADPH, 25 nM GSR and 400 μM GSH) for 10 min before analysis by HPLC. Over this period, all the SeMetO was consumed, with a concomitant increase (200 μM) in the SeMet concentration, consistent with rapid reduction of SeMetO by GSH and recycling with the GSR/NADPH system (data not shown). Analogous experiments could not be performed with SeTalO, as components of the GSR system co-elute with SeTalO and SeTal (data not shown).

3.5. N-Chloramine consumption in SeMet/SeTal supplemented enzymatic reduction systems

The effect of SeMet and SeTal on the rate of TrxR reduction of a series of N-chloramines was examined, as these oxidants react rapidly with SeMet and SeTal to form selenoxides [11]. Chloramines were formed on taurine (TauCl), N-α-acetyllysine (LysCl) and glycine (GlyCl)

by reaction of the parent amine (10 mM) with HOCl (2 mM) before dilution (200 μM chloramine) and addition to NADPH (700 μM) and TrxR (25 nM) in the presence or absence of SeMet or SeTal (20 or 200 μM). The absorbance was monitored for 2 h at 340 nm and the rate of NADPH consumption determined by fitting a straight line to the initial 25 min of absorbance data (Fig. 7, Supplementary material Fig. S4). With TauCl, the rate of NADPH consumption was similar in the presence and absence of TrxR (Fig. 7a and b). Reaction of TauCl with SeMet or SeTal (20–200 μM) resulted in a significant, dose-dependent, decrease in the rate of NADPH consumption observed (Fig. 7b). Similar results were obtained with LysCl and GlyCl (Supplementary material Fig. S4). SeTal (200 μM) reduced the rate of NADPH consumption seen with TauCl to the same rate as controls, whereas SeMet (200 μM) reduced the rate of NADPH consumption to that observed after the addition of pre-formed SeMetO to the TrxR system (see Fig. 5). These data are consistent with competition of SeMet/SeTal and NADPH/TrxR for the N-chloramines, with subsequent TrxR-mediated reduction of the resulting selenoxides, in the case of SeMet.

The concentrations of SeMet, SeMetO, SeTal and SeTalO were assessed by HPLC 20 min and 2 h after the addition of TauCl to the NADPH (700 μM), TrxR (25 nM) system supplemented with SeMet or SeTal (200 μM) (Fig. 7c). After 20 min, the major species detected were the selenoxides (164 ± 8 μM SeMetO and 175 ± 6 μM SeTalO). After 2 h, the concentration of SeMetO decreased to 12 ± 13 μM, with a corresponding increase observed in SeMet levels, which has been attributed to SeMetO reduction by TrxR (Fig. 7c). In contrast, SeTalO levels were unchanged, reflecting the inability of TrxR to reduce SeTalO (Fig. 7d).

These studies were extended to examine the effect of SeMet and
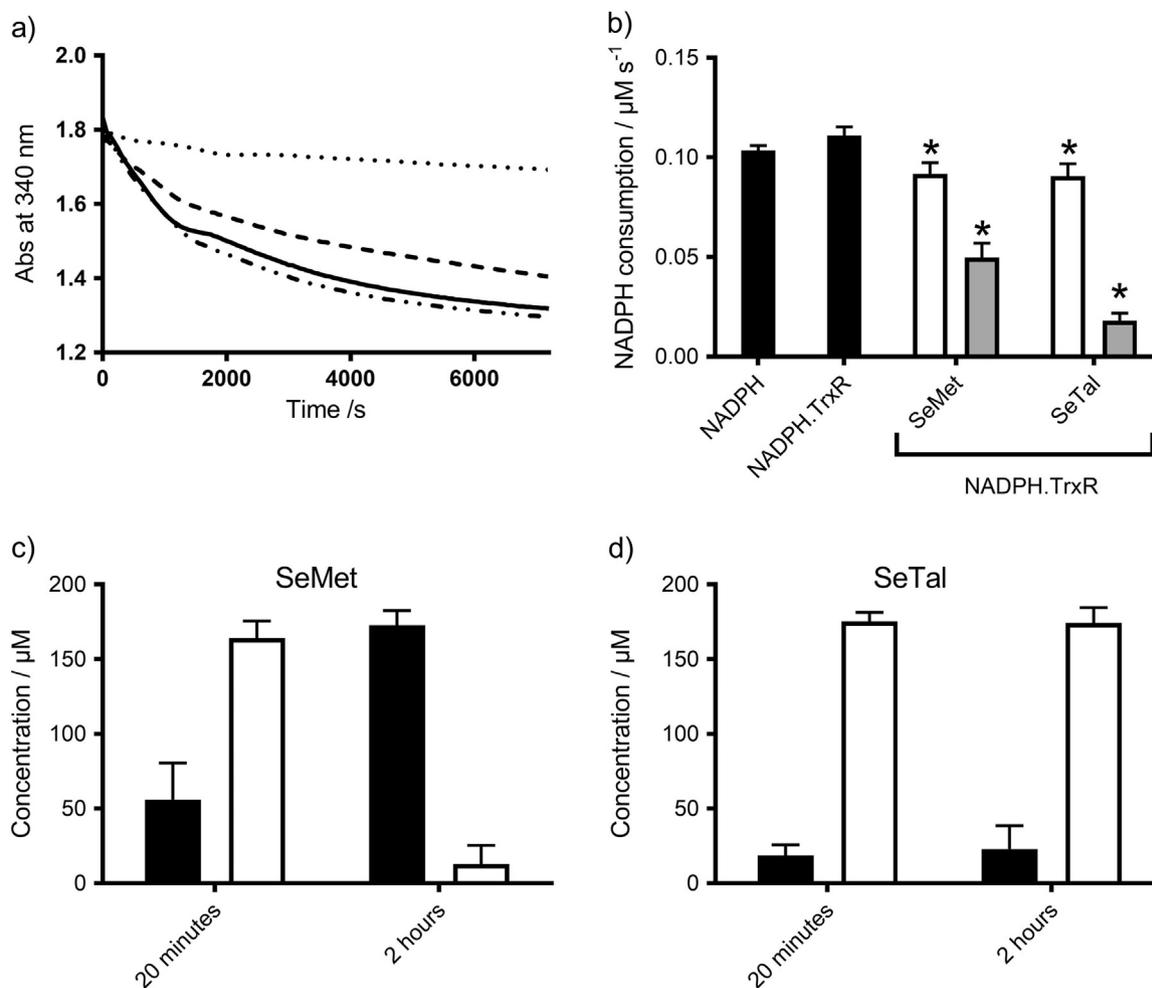
Fig. 7. Reduction of *N*-chloramines by the TrxR system in the presence of SeMet or SeTal. Panel (a) shows typical absorbance decrease of NADPH observed at 340 nm over time on addition of TauCl (200 μM) to NADPH (700 μM; solid line) in the presence of TrxR (25 nM; dot-dashed line) and SeMet (200 μM; dashed line) or SeTal (200 μM; dotted line). Panel (b) shows the rate of consumption of NADPH measured by fitting a straight line to the first 25 min of the data presented in (a), with data from experiments performed with 20 μM (white bars) and 200 μM (grey bars) SeMet and SeTal. Panel (c) shows the recovery of SeMet (black bars) from SeMetO (white bars) as determined by HPLC after TauCl was added to TrxR/NADPH in the presence of 200 μM SeMet. Panel (d) is as (c) but with SeTal. For panels (b)–(d), data represent mean ± SD from 3 independent experiments. * Indicates significant difference (p < 0.05) from the control by one-way ANOVA with Tukey's post-hoc test.

SeTal addition on the rate of *N*-chloramine reduction by the GSR system. In this case, TauCl, LysCl or GlyCl (200 μM) were mixed by stopped flow apparatus with NADPH (500 μM), GSR (25 nM), and GSH (400 μM) in the presence or absence of SeMet or SeTal (20 or 200 μM). The rate of consumption of NADPH was determined by fitting a straight line to the absorbance data obtained 2–10 s after mixing. A time-dependent decrease in NADPH absorbance at 340 nm was observed on mixing TauCl, LysCl or GlyCl with the components of the GSR system (Fig. 8, Supplementary material Fig. S5). In the presence of SeMet (200 μM), a significant increase in the rate of NADPH consumption was observed compared to that seen with TauCl alone (Fig. 8b). A similar, but non-significant, trend was observed with SeTal. However, there was no change in the rate of NADPH consumption mediated by the GSR system in the presence or absence of SeMet and SeTal in experiments with LysCl and GlyCl (Supplementary material Fig. S5).

The concentrations of SeMet and SeMetO were assessed by HPLC 10 min after addition of TauCl, LysCl and GlyCl (200 μM) to NADPH (500 μM), GSR (25 nM), and GSH (400 μM) in the presence of SeMet (200 μM). Under these conditions, no SeMetO was detected, with complete recovery of SeMet observed (Fig. 8c). These data suggest that for TauCl at least, the presence of SeMet may be able to enhance the reduction of the *N*-chloramine by the GSR system via formation of a selenoxide.

4. Discussion

In this study, we show that the selenoxides formed on SeMet, SeTal and other Se compounds are rapidly reduced by endogenous low-molecular mass thiols. We also provide evidence for enzymatic reduction of SeMetO, but not SeTalO, by the TrxR/NADPH system, whereas both selenoxides were rapidly reduced by a GSR/NADPH system. The rapid enzymatic reduction of SeMetO also allowed SeMet to promote the reduction of *N*-chloramines.

We show that GSH is capable of reducing SeMetO to SeMet with concomitant formation of GSSG, consistent with previous studies [14,15]. Reduction of SeMetO or SeTalO by GSH occurs with similar stoichiometries, with 1 mol of selenoxide consumed and 1 mol of parent selenoether recovered for every 2 mol of GSH. The kinetic analysis supports a two-step reaction mechanism, where one thiol reacts with the selenoxide to form a selenosulfide with rate constant k_1. This intermediate then reacts with a second thiol to give the disulfide and selenoether, with rate constant k_2 (Scheme 1). This process is more clearly observed on reaction of SeMetO with GSH, where an initial rapid decrease in absorbance (at 240 nm) is observed, corresponding to the first reaction, followed by a slower increase in absorbance, attributed to the second reaction (Fig. 4d). The derived rate constant, k_2, for the second step ($\sim 10^4 \, M^{-1} \, s^{-1}$) is an order of magnitude lower than k_1 for the first step for SeMetO with GSH (Table 1). This results in

a)

b)
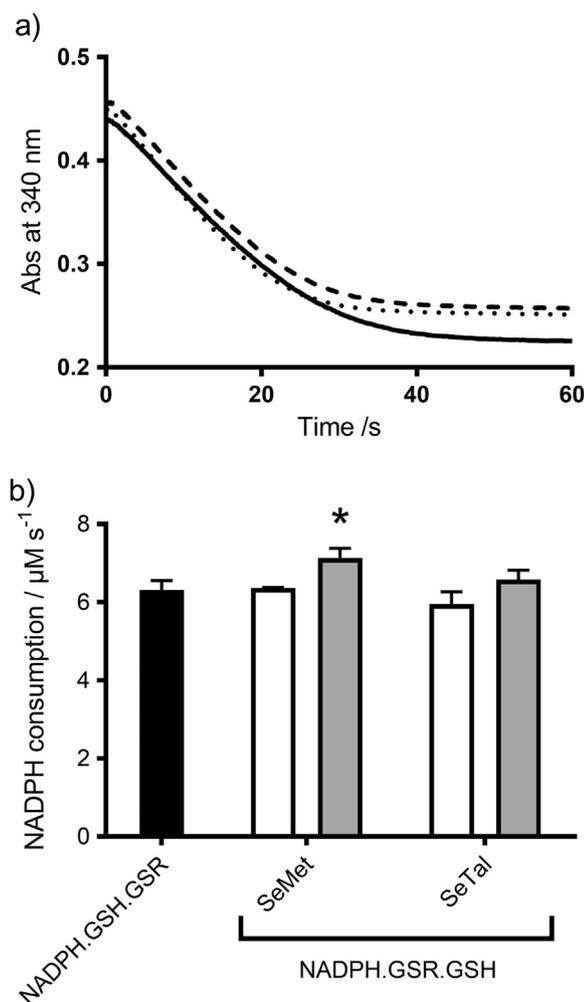
Fig. 8. Reduction of chloramines by the GSR system in the presence of SeMet or SeTal. Panel (a) shows the typical decrease of NADPH measured at 340 nm over time on addition of TauCl (200 μM; solid line), to GSR (25 nM), GSH (400 μM) and NADPH (500 μM) in the presence of SeMet (200 μM; dashed line) or SeTal (200 μM; dotted line) using a stopped-flow system with 2 mm path length cell. Panel (b) shows the initial rate of absorbance decrease over the first 10 s of data represented in (a), with data from experiments performed with 20 μM (white bars) and 200 μM (grey bars) SeMet and SeTal. For panel (b), data represent mean ± SD from 3 independent experiments. * Indicates significant difference (p < 0.05) from the control by one-way ANOVA with Tukey's post-hoc test.

kinetic traces that have two distinct first order phases, which is consistent with both phases being dependent on the thiol concentration that is present in excess (Fig. S3). The data obtained for the other selenoxides are consistent with this mechanism, assuming that the rate constant k_2 for the second step is significantly greater than k_1 for the first step, resulting in rapid reaction of the intermediate and kinetic traces that appear first order with only a single phase. It is also possible that a mechanism involving a fast equilibrium between the selenoxide and selenosulfide could play a role.

A selenosulfide has been proposed as an intermediate in the reactions of selenoxides with thiols. However, these intermediates have not been characterized, as selenosulfides react rapidly with thiols to give disulfides and selenols as products [28]. This disulfide exchange mechanism is analogous to that of TrxR [29]. Similar intermediates have been proposed in the reduction of methionine sulfoxide (MetSO) by Se-containing methionine sulfoxide reductase (Msr) enzymes [29–31]. Previously published rate constants for reaction of low-molecular mass thiols with selenosulfides have been obtained from extrapolation of experimental data based on thermodynamic calculations, with the rate constant for reaction of DTT with hemi-selenocys-

tine reported as $\sim 10\,M^{-1}\,s^{-1}$ [28]. In contrast the rate constant determined here for the second step of the SeMetO reaction with GSH is $\sim 10^4\,M^{-1}\,s^{-1}$. During selenoxide reduction, the selenosulfide intermediate is proposed to retain the oxygen bound to Se (Scheme 1, Compound B). This electronegative oxygen atom bound to the Se centre may contribute to the electrophilicity of the Se atom by withdrawing electrons, leading to a more rapid nucleophilic reaction of the second thiol [28]. Similarly, the reaction of the Sec catalytic domain of TrxR with active thioredoxin occurs with k 10^7–$10^8\,M^{-1}\,min^{-1}$ [32,33], though this high value is likely to reflect the influence of the surrounding protein structure and microenvironment [28].

Evidence has also been obtained for the enzymatic reduction of selenoxides by TrxR and GSR in the presence of NADPH. The TrxR system reduces SeMetO, but not SeTalO, whereas the GSR system rapidly reduces both SeMetO and SeTalO. This may be related to an influence of the selenosugar structure on the kinetics, as the reaction should be thermodynamically favourable, given the higher reduction potential of selenols compared to thiols. SeTalO may be subject to steric hindrance in accessing the active site of TrxR, though the active site of TrxR is on a flexible tail [34]. However, if the site of reduction of SeMetO in TrxR is the N-terminal Cys-X-X-Cys redox centre [34], rather than the active site selenol, this may limit the accessibility of SeTalO for reduction. With GSR, reduction occurs after an initial lag phase (< 1 s), attributed to the formation of GSSG by the reaction of the SeMetO and SeTalO with GSH. The GSSG is then reduced by GSR, resulting in the consumption of NADPH. The rate of NADPH consumption was more rapid with GSR than TrxR, consistent with the former enzyme system being the more likely mechanism for selenoxide repair in vivo.

The addition of Trx to the TrxR/NADPH/SeMetO system did not increase the rate of selenoxide reduction, in contrast to previous reports [21]. This may reflect differences in the concentration and type of Trx used, though addition of Trx together with GPx, MsrA or MsrB2 was also unable to increase the rate at which NADPH was consumed upon addition of SeMetO or SeTalO. This could reflect that the reduction of TrxR by NADPH is the limiting factor in the reduction cycle, such that NADPH consumption is not increased with the addition of coupled enzymatic systems. However, this may be unlikely given that other Trx/TrxR/NADPH-dependent reactions proceed more rapidly under analogous conditions. Thus, an alternative explanation is that the kinetics of the reaction of SeMetO with TrxR may be greater than that observed for the other enzymes, with TrxR preferentially reducing SeMetO directly.

We also show that N-chloramines can be reduced enzymatically via the TrxR and GSR systems, which results in the consumption of NADPH. In this case, a time-dependent decrease in NADPH concentration, due to the direct reaction of NADPH with N-chloramines, is also observed in the absence of TrxR and GSR. These data agree with previous studies, where the reaction of NADPH with various N-chloramines occurs with k~$1\,M^{-1}\,s^{-1}$ [35,36], and results in the formation of a chlorinated NADPH product that is toxic to cells [37]. Addition of SeMet or SeTal lowered the NADPH consumption rate after addition of N-chloramines to NADPH and TrxR to a rate similar to that observed in the selenoxide reduction experiments. This reflects reaction of N-chloramines with SeMet and SeTal, followed by the slower reduction of the resulting selenoxide (or no reduction as with SeTalO). This is achieved on addition of SeMet/SeTal at concentrations equimolar to that of the N-chloramine, in the presence of an excess (3.5-fold) of NADPH. Detoxification of the N-chloramine via this pathway would also be expected to decrease formation of the toxic chlorinated NADPH product, and subsequently increase cellular NADP$^+$. Rapid reduction of the model N-chloramines was also observed with the GSR system, which for TauCl at least, increased in the presence of SeMet. This may be related to the lower rate constant for reaction of this N-chloramine with GSH [13]. Taken together, these data suggest that the addition of selenium compounds will have a limited capacity to increase detoxification of N-chloramines via this pathway.

The ability of other selenium compounds, such as ebselen and

selenocystamine, to enhance oxidant scavenging has previously been reported, though these function via a different mechanism to that discussed here [22,38,39]. It is proposed that the redox enzymes, including Trx and GSR, reduce the diselenides or ebselen to a selenol group, which then rapidly reacts with the oxidant to reform the parent compound [22,38,39]. Ebselen was more effective at oxidant removal in conjunction with the Trx system compared to the GSR system [39], while the opposite was observed for SeMet and SeTal. This is consistent with the differing mechanism proposed for SeMet and SeTal, where the parent species react directly with the oxidant to form selenoxides, followed by reduction by the enzymes or GSH to reform the parent compound.

In summary, we have defined the rate constants for reaction of SeMetO and SeTalO with GSH and other thiols, and demonstrated the potential for other endogenous antioxidant systems, including GSR and TrxR, to recycle these intermediates to the parent selenium species. The ability of selenium-containing compounds such as SeMet and SeTal to prevent oxidative damage in vivo will however, be dependent on the levels of these species that can be achieved on supplementation. Given that the rate constants for reaction of selenium-containing compounds with oxidants, including MPO-derived species, are in general 10–100-fold greater than for the analogous reactions with thiol-containing compounds (e.g. HOSCN [8,40], N-chloramines [11,13]), lower concentrations of SeMet/SeTal should be able to compete with other biological targets, including thiols. This is supported by recent in vivo studies in SeTal supplemented, atherosclerosis-prone apoE$^{-/-}$ mice, where plasma levels of SeTal of 5–10 µM were achieved on supplementation with non-toxic doses of SeTal, which is only slightly below plasma GSH levels (10–15 µM) with LC-MS/MS data demonstrating the formation of SeTalO on prolonged incubation of the isolated plasma resulting from autoxidation reactions (Zacharias et al., unpublished). However, further in vivo studies are required to determine the therapeutic potential of SeMet and SeTal to mitigate oxidative damage during chronic inflammation and assess the subsequent effects on the extent of disease development.

Acknowledgements

Appendix A. Supplementary material

Supplementary data associated with this article can be found in the online version at http://dx.doi.org/10.1016/j.redox.2017.04.023.

References

[1] M.J. Davies, C.L. Hawkins, D.I. Pattison, M.D. Rees, Mammalian heme peroxidases: from molecular mechanisms to health implications, Antioxid. Redox Signal. 10 (2008) 1199–1234.

[2] M.B. Hampton, A.J. Kettle, C.C. Winterbourn, Inside the neutrophil phagosome: oxidants, myeloperoxidase, and bacterial killing, Blood 92 (1998) 3007–3017.

[3] B.S. Rayner, D.T. Love, C.L. Hawkins, Comparative reactivity of myeloperoxidase-derived oxidants with mammalian cells, Free Radic. Biol. Med. 71 (2014) 240–255.

[4] E.L. Thomas, M.B. Grisham, M.M. Jefferson, Preparation and characterization of chloramines, Methods Enzymol. 132 (1986) 569–585.

[5] S.J. Klebanoff, Myeloperoxidase: friend and foe, J. Leukoc. Biol. 77 (2005) 598–625.

[6] T. Lazarevic-Pasti, A. Leskovac, V. Vasic, Myeloperoxidase inhibitors as potential drugs, Curr. Drug Metab. 16 (2015) 168–190.

[7] S. Padmaja, G.L. Squadrito, J.N. Lemercier, R. Cueto, W.A. Pryor, Rapid oxidation of DL-selenomethionine by peroxynitrite, Free Radic. Biol. Med. 21 (1996) 317–322.

[8] O. Skaff, D.I. Pattison, P.E. Morgan, R. Bachana, V.K. Jain, K.I. Priyadarsini, M.J. Davies, Selenium-containing amino acids are targets for myeloperoxidase-derived hypothiocyanous acid: determination of absolute rate constants and implications for biological damage, Biochem. J. 441 (2012) 305–316.

[9] C. Storkey, M.J. Davies, D.I. Pattison, Reevaluation of the rate constants for the reaction of hypochlorous acid (HOCl) with cysteine, methionine, and peptide derivatives using a new competition kinetic approach, Free Radic. Biol. Med. 73 (2014) 60–66.

[10] C. Storkey, D.I. Pattison, J.M. White, C.H. Schiesser, M.J. Davies, Preventing protein oxidation with sugars: scavenging of hypohalous acids by 5-selenopyranose and 4-selenofuranose derivatives, Chem. Res. Toxicol. 25 (2012) 2589–2599.

[11] L. Carroll, D.I. Pattison, S. Fu, C.H. Schiesser, M.J. Davies, C.L. Hawkins, Reactivity of selenium-containing compounds with myeloperoxidase-derived chlorinating oxidants: second-order rate constants and implications for biological damage, Free Radic. Biol. Med. 84 (2015) 279–288.

[12] D.I. Pattison, M.J. Davies, Absolute rate constants for the reaction of hypochlorous acid with protein side chains and peptide bonds, Chem. Res. Toxicol. 14 (2001) 1453–1464.

[13] A.V. Peskin, C.C. Winterbourn, Kinetics of the reactions of hypochlorous acid and amino acid chloramines with thiols, methionine, and ascorbate, Free Radic. Biol. Med. 30 (2001) 572–579.

[14] A. Assmann, K. Briviba, H. Sies, Reduction of methionine selenoxide to selenomethionine by glutathione, Arch. Biochem. Biophys. 349 (1998) 201–203.

[15] R.J. Krause, A.A. Elfarra, Reduction of L-methionine selenoxide to seleno-L-methionine by endogenous thiols, ascorbic acid, or methimazole, Biochem. Pharmacol. 77 (2009) 134–140.

[16] B. Gammelgaard, C. Cornett, J. Olsen, L. Bendahl, S.H. Hansen, Combination of LC-ICP-MS, LC-MS and NMR for investigation of the oxidative degradation of selenomethionine, Talanta 59 (2003) 1165–1171.

[17] R.J. Krause, S.C. Glocke, A.R. Sicuri, S.L. Ripp, A.A. Elfarra, Oxidative metabolism of seleno-L-methionine to L-methionine selenoxide by flavin-containing monooxygenases, Chem. Res. Toxicol. 19 (2006) 1643–1649.

[18] F. Kumakura, B. Mishra, K.I. Priyadarsini, M. Iwaoka, A water-soluble cyclic selenide with enhanced glutathione peroxidase-like catalytic activities, Eur. J. Org. Chem. (3) (2010) 440–445.

[19] K. Arai, F. Kumakura, M. Takahira, N. Sekiyama, N. Kuroda, T. Suzuki, M. Iwaoka, Effects of ring size and polar functional groups on the glutathione peroxidase-like antioxidant activity of water-soluble cyclic selenides, J. Org. Chem. 80 (2015) 5633–5642.

[20] I. Carlberg, B. Mannervik, Glutathione-reductase, Methods Enzymol., 113, 1985, pp. 484–490.

[21] A.S. Rahmanto, M.J. Davies, Catalytic activity of selenomethionine in removing amino acid, peptide, and protein hydroperoxides, Free Radic. Biol. Med. 51 (2011) 2288–2299.

[22] M. Bjornstedt, S. Kumar, A. Holmgren, Selenodiglutathione is a highly efficient oxidant of reduced thioredoxin and a substrate for mammalian thioredoxin reductase, J. Biol. Chem. 267 (1992) 8030–8034.

[23] M. Bjornstedt, M. Hamberg, S. Kumar, J. Xue, A. Holmgren, Human thioredoxin reductase directly reduces lipid hydroperoxides by NADPH and selenocystine strongly stimulates the reaction via catalytically generated selenols, J. Biol. Chem. 270 (1995) 11761–11764.

[24] J.C. Morris, Acid ionization constant of HOCl from 5 to 35 degrees, J. Phys. Chem. 70 (1966) 3798–3805.

[25] C. Storkey, M.J. Davies, J.M. White, C.H. Schiesser, Synthesis and antioxidant capacity of 5-selenopyranose derivatives, Chem. Commun. 47 (2011) 9693–9695.

[26] C.L. Hawkins, P.E. Morgan, M.J. Davies, Quantification of protein modification by oxidants, Free Radic. Biol. Med. 46 (2009) 965–988.

[27] P. Eyer, F. Worek, D. Kiderlen, G. Sinko, A. Stuglin, V. Simeon-Rudolf, E. Reiner, Molar absorption coefficients for the reduced Ellman reagent: reassessment, Anal. Biochem. 312 (2003) 224–227.

[28] D. Steinmann, T. Nauser, W.H. Koppenol, Selenium and sulfur in exchange reactions: a comparative study, J. Org. Chem. 75 (2010) 6696–6699.

[29] R.J. Hondal, S.M. Marino, V.N. Gladyshev, Selenocysteine in thiol/disulfide-like exchange reactions, Antioxid. Redox Signal. 18 (2013) 1675–1689.

[30] A. Olry, S. Boschi-Muller, M. Marraud, S. Sanglier-Cianferani, A. Van Dorsselear, G. Branlant, Characterization of the methionine sulfoxide reductase activities of PILB, a probable virulence factor from Neisseria meningitidis, J. Biol. Chem. 277 (2002) 12016–12022.

[31] S. Boschi-Muller, A. Olry, M. Antoine, G. Branlant, The enzymology and biochemistry of methionine sulfoxide reductases, Biochim. Biophys. Acta 1703 (2005) 231–238.

[32] L.W. Zhong, A. Holmgren, Essential role of selenium in the catalytic activities of mammalian thioredoxin reductase revealed by characterization of recombinant enzymes with selenocysteine mutations, J. Biol. Chem. 275 (2000) 18121–18128.

[33] B.E. Eckenroth, B.M. Lacey, A.P. Lothrop, K.M. Harris, R.J. Hondal, Investigation of the C-terminal redox center of High-M-r thioredoxin reductase by protein engineering and semisynthesis, Biochemistry 46 (2007) 9472–9483.

[34] L.W. Zhong, E.S.J. Arner, A. Holmgren, Structure and mechanism of mammalian thioredoxin reductase: the active site is a redox-active selenolthiol/selenenylsulfide formed from the conserved cysteine-selenocysteine sequence, Proc. Natl. Acad. Sci. USA 97 (2000) 5854–5859.

[35] W.A. Prutz, R. Kissner, W.H. Koppenol, H. Rueegger, On the irreversible destruction of reduced nicotinamide nucleotides by hypohalous acids, Arch. Biochem. Biophys. 380 (2000) 181–191.

[36] W.A. Prutz, Interaction of hypochlorous acid with pyrimidine nucleotides, and secondary reactions of chlorinated pyrimidines with GSH, NADH, and other substrates, Arch. Biochem. Biophys. 349 (1998) 183–191.

[37] B.W. Griffin, R. Haddox, Chlorination of NADH – similarities of the HOCl-supported and chloroperoxidase-catalyzed reactions, Arch. Biochem. Biophys. 239 (1985) 305–309.

[38] R. Zhao, A. Holmgren, A novel antioxidant mechanism of ebselen involving ebselen diselenide, a substrate of mammalian thioredoxin and thioredoxin reductase, J. Biol. Chem. 277 (2002) 39456–39462.

[39] R. Zhao, H. Masayasu, A. Holmgren, Ebselen: a substrate for human thioredoxin reductase strongly stimulating its hydroperoxide reductase activity and a superfast thioredoxin oxidant, Proc. Natl. Acad. Sci. USA 99 (2002) 8579–8584.

[40] O. Skaff, D.I. Pattison, M.J. Davies, Hypothiocyanous acid reactivity with low-molecular-mass and protein thiols: absolute rate constants and assessment of biological relevance, Biochem. J. 422 (2009) 111–117.